Terahertz absorption by cellulose: Application to ancient paper artifacts

Article (Supplemental Material)

Supplemental Material for: Precise determination of cellulose Terahertz absorption: application to ancient paper artifacts

M. Peccianti[1], R. Fastampa[2,3], A. Mosca Conte[4], O. Pulci[4], C. Violante[4], J. Łojewska[5], M. Clerici[6], R. Morandotti[7,8,9], and M. Missori[3*]

[1] *Emergent Photonics Lab (EPic) - Dept. of Physics and Astronomy, University of Sussex, BN1 9QH Brighton UK*

[2] *Dipartimento di Fisica, Università di Roma "Sapienza", Roma, Italy*

[3] *Istituto dei Sistemi Complessi, Consiglio Nazionale delle Ricerche, UOS Sapienza, Roma, Italy*

[4] *ETSF, Dipartimento di Fisica, Universitá di Roma Tor Vergata, Rome, Italy*

[5] *Faculty of Chemistry, Jagiellonian University, Ingardena 3, 30-060 Krakow, Poland*

[6] *School of Engineering, University of Glasgow, G12 8LT, Glasgow, UK*

[7] *INRS-EMT, University of Quebec, Varennes, Quebec J3X 1S2, Canada*

[8] *Institute of Fundamental and Frontier Sciences, University of Electronic Science and Technology of China, Chengdu 610054, China and*

[9] *National Research University of Information Technologies, Mechanics and Optics, St. Petersburg, Russia*

I. EXPERIMENTAL DETAILS

A. THz TDS set-up

The THz spectra were acquired in the transmission mode by using a Menlo Systems TERA K15 Terahertz Time Domain Spectrometer (THz-TSD) equipped with photoconductive antennae. For all the acquisitions, the time scan range was set to $100ps$ and the data were collected with a time resolution of $30fs$. The usable spectral range, i.e. where data are reliable, was found to be 0.2–3.5 THz. The frequency dependent dynamic range was about 80 dB at 0.35 THz and about 20 dB at 3.5 THz. The signal was averaged over all the scans for a time of 200s (1400 scans). The THz radiation emitted by the photoconductive antenna was collected and focused onto the sample using of two TPX lenses with 50 mm nominal focal length. The radiation transmitted through the sample was collected and focused onto the detector antenna by another couple of identical 50 mm nominal focal length TPX lenses. The samples were measured out of the THz focus, so that the THz pulse could probe a large area, thus minimizing heterogeneity related effects. The samples were displaced towards the detector antenna until the illuminated area was approximately 4 mm in diameter(approximately 6 mm away from the THz focus). Since the water vapor absorbs THz radiation, the sample compartment of the spectrometer was purged with dry N_2 until the water vapor absorption lines became indistinguishable from noise up to 3.0 THz (corresponding to nearly 60 min of purging time before spectra acquisition).

B. Samples details

The paper samples consist of a random assembly of cellulose fibers and voids, in a sample dependent relative concentration. Typical sizes of fibers and voids are around 10-20 μm, i.e. much smaller than the wavelengths associated to the 0.2–3.5 THz range (i.e., from 1500 μm to 86 μm). Therefore, THz radiation probes the volume averaged properties of the papers sheets. To recover the refractive index and the absolute absorption coefficient of cellulose fibers at THz frequencies, it is necessary to estimate the relative amount of cellulose in the paper sheets. This information can be recovered from the paper sample density,

$$\rho_{paper} = \frac{w}{t\,\Sigma}$$

by measuring their mean thickness values (t), surface area (Σ) and weight (w).

Due to the production process, the paper sheets present variable thicknesses. To estimate a mean value t, the thickness was measured in several different positions (typically more than 10) by using a paper-gauging micrometer (with sensitivity of $10\mu m$) equipped with a spherical probe (diameter 2 mm) on one side and a metallic plate with a diameter of 19 mm on the other side. The measuring force between the two probes was set to 0.1 N.

The mean thickness values are reported in Table I.

The thicknesses values required to remove the FP oscillations in the algorithm are within $t \pm 10\mu m$, proving a good estimation for the paper samples' thickness.

The weights w of the paper sheets were measured using a laboratory scale (Sartorius Research R200D) with a sensitivity of 10^{-5}g. Both thickness and weight measurements were carried out at a temperature of $(21 \pm 1)°C$ and a relative humidity RH=(56 ± 2)%. In these environmental conditions, a small amount (around 5-7% in weight) of water in the paper sheets (moisture content) is to be expected due to the hydrophilic character of cellulose [1]. This uncertainty in weight affects the samples density values.

The surface areas Σ of the samples were measured by acquiring their images using a calibrated imaging flatbed

Samples	$t(\mu m)$	$\rho_{paper}(g/cm^3)$	v
P2V	90	0.84	0.56
A1	108	0.76	0.51
B1	102	0.71	0.47
A3	75	0.71	0.47
N1	124	0.91	0.61

Table I. Mean thickness (t), densities (ρ_{paper}) and volume fractions (v) of the modern and ancient specimens measured in the experiments. The samples belonging to the P2V series (aged and not aged) show the same thickness within the experimental errors. Details on the parameters are reported in the text.

scanner.

ρ_{paper} was then estimated assuming $\rho_{paper} = w/t_{mean}\,\Sigma$. The results for ρ_{paper} are reported in Table I. The relative error in ρ_{paper} is about 10%, essentially due to the uncertainty in the measurement of t and w, the last due to the unknown moisture content. The volume fraction v of cellulose fibers in the sample can be obtained by assuming $v = V_c/V_{paper} = \rho_{paper}/\rho_c$, where V_c and V_{paper} are the volume occupied by cellulose fibers and the volume of the paper sheets used in this study, respectively, while $\rho_c = 1.5 g/cm^3$ is the average density of cellulose fibers. The values of v for the samples studied are reported in Table I.

Such numbers are required to calculate the absolute absorption coefficient (α) and the refractive index (n) of cellulose fibers, given that THz radiation probes the volume averaged properties of the papers sheets [2–4]:

$$n_{paper} = (1 - v)\, n_a + v\, n \tag{1}$$

$$\alpha_{paper} = (1 - v)\, \alpha_a + v\, \alpha \tag{2}$$

Here n_{paper} and α_{paper} are the refractive index and absolute absorption coefficient obtained for the paper sheets while n_a, and α_a are the refractive index and absolute absorption coefficient of dry N_2 (assumed to be $n_a = 1$ and $\alpha_a = 0$ in our THz measuring range). Therefore:

$$n = \frac{n_{paper} - (1 - v)}{v} \tag{3}$$

$$\alpha = \frac{\alpha_{paper}}{v} \tag{4}$$

The modern samples, named P2REF (unaged) and P2Vx where x = 06, 12, 24 and 47, were sourced from the Netherlands Organization for Applied Scientific Research (TNO). They are made from unbleached cotton linters and contain very little inorganic material (ash content <0.005% in weight) and no additives or lignin [5, 6]. Note that the samples named P2Vx were artificially aged at a temperature of $90°C$ for x days in humid air (RH 59%) inside a closed vessel. Under these conditions, and beside high temperature, the expected degradation factors are air, water vapor and the volatile products of cellulose degradation [7, 8]. The aging conditions used here were chosen in order to produce measurable changes in the THz spectra of the model paper samples within a reasonable time frame. At the chosen temperature of $90°C$, a moderate degradation of the cellulose polymers is expected [5, 7, 8].

C. DFT Computational details

Cellulose has been modeled as a crystal in its most common crystalline form (I_β phase), as in Refs. [2–4]. Both the unit cell and the atomic coordinates of the structures used in those references have been relaxed by using a density-functional-theory plane-wave code with ultrasoft pseudopotentials (QUANTUM ESPRESSO [9]). For the unaged cellulose theoretical unit cell, we obtained the following Bravais vectors expressed in Bohr: (19.31, -0.1494, 0.6432), (-0.1353, 15.19, -0.3923), and (0.1847, 8.144, 8.051). In order to include Van der Waals (VdW) interactions in the total energy calculation, a VdW-DF2 [10] nonlocal density functional has been employed. This functional is an enhanced version of VdW-DF [11] and it is based on a more accurate semilocal exchange functional, the PW86 [12]. It was chosen to achieve a better description of the H-bonds [13]. A cutoff of 40 Ry for the Kohn-Sham wavefunctions and of 800 Ry for the charge density was employed. Proper ultrasoft pseudopotentials [14], conveniently generated [15] to be suitable for the nonlocal VdW functionals, were used. The Irreducible Brillouin Zone has been sampled with 14 k-points [2–4]. Vibrational properties have been calculated using finite displacements within the DFT framework, as described in Ref. [16]. We applied this approach for the calculation of the phononic eigenvalues and eigenfunctions at the Γ-point, to determine the cellulose THz absorption spectrum in its pristine form.

D. Extraction algorithm details

The analysis of the THz-TDS transmission mode signals can be carried out by using the complex transfer function $\hat{T}(\omega)$:

$$\hat{T}(\omega) = T(\omega)\, e^{i\,\varphi(\omega)} = \frac{\hat{E}_{sample}(\omega)}{\hat{E}_{ref}(\omega)} \tag{5}$$

where $\hat{E}_{sample}(\omega)$ and $\hat{E}_{ref}(\omega)$ are the spectral amplitude and phase with and without the sample in the THz line, respectively [17]. The frequency dependent behavior of

the complex refraction index $\hat{n}(\omega) = n(\omega) + i\alpha(\omega)\, c/2\omega$ (n is the real refraction index and α the absorption coefficient) can be extracted from the measured $\hat{T}(\omega)$ using a simple analytical approach for samples with particular constraints in terms of thickness and refractive index [18, 19]. In this case, it is possible to disregard, in the solution of the electromagnetic problem, the Fabry–Perot effect arising from the multiple reflections occurring inside the sample.

Under such conditions one obtains:

$$T(\omega)\, e^{i\,\varphi(\omega)} = \frac{4n}{(1+n)^2} e^{-\alpha d/2} e^{i\,(n-1)\omega d/c} \tag{6}$$

Eq. 6 can be easily inverted in order to derive the optical parameters:

$$n(\omega) = 1 + \frac{\varphi(\omega) c}{\omega d} \tag{7}$$

$$\alpha(\omega) = -2/d \ln\left(\frac{(1+n)^2}{4n} T(\omega)\right) \tag{8}$$

On the contrary, the analysis of the THz-TDS signals measured on optically thin, low refractive index samples is more complicated because a new term in the transfer function must be considered to account for the FP effect. In this case, multiple reflections have to be included in the solution of the electromagnetic problem. In fact if the Eqs. 7 and 8 are still used, fictitious oscillations appear in the optical parameters (see Figs.1 and 2).

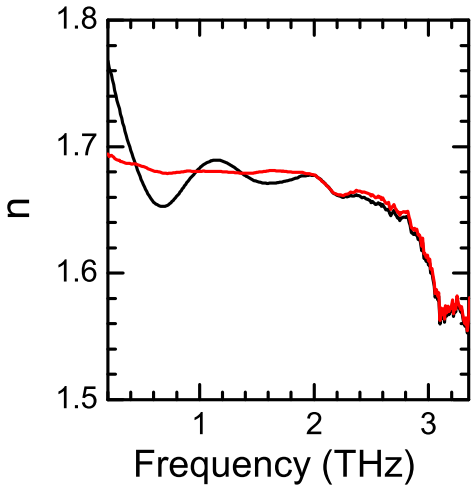

Figure 1. Refraction index of the cellulose fibers of sample A1 without (red) and with (black) removal of the FP oscillations.

However, if the *FP*-term is considered, the analytical expression of the transfer function that is at the basis

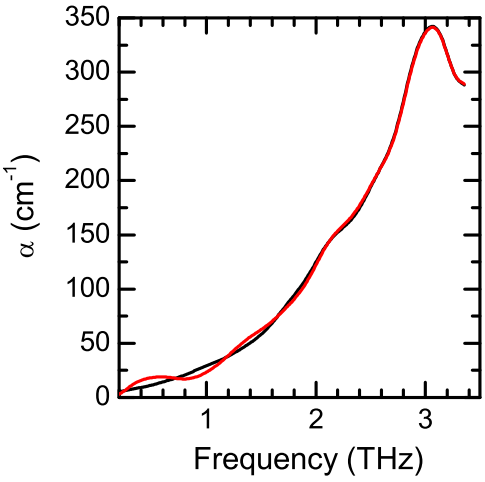

Figure 2. Absorption coefficient curves of the cellulose fibers of sample A1 without (red) and with (black) removal of the FP oscillations.

of the extraction method used to determine the complex refraction index is much more complicated and can be solved only numerically. In this case, the resulting transfer function expression is:

$$\hat{T}(\omega) = \frac{4\hat{n}}{(1+\hat{n})^2} \frac{e^{i\,(\hat{n}-1)\omega d/c}}{FP(\hat{n},\omega)} \tag{9}$$

where $FP(\hat{n},\omega)$ is the function giving the *FP* contribution:

$$FP(\hat{n},\omega) = 1 - \left(\frac{\hat{n}-1}{\hat{n}+1}\right)^2 e^{-\alpha\, d} e^{2in\,\omega d/c}$$

Naming:

$$f(\hat{n}) = \hat{T}_{exp}(\omega) - \frac{4\hat{n}}{(1+\hat{n})^2} \frac{e^{i\,(\hat{n}-1)\omega d/c}}{FP(\hat{n},\omega)} \tag{10}$$

as the difference between the theoretical and experimental transfer function, we have to find the $\hat{n}$ complex root that satisfy the equation: $f(\hat{n},\omega_j) = 0$, for each ω_j. To recover the spectral behavior of the complex refractive index in paper sheets we have developed a signal extraction procedure optimized for thin absorbent samples of low refractive index. In particular, it has been necessary to minimize the instrumental errors involved in the determination of the subtle time difference between the reference and the sample pulses ($\sim$ 100fs). The overall convergence error associated to the procedure can be estimated by considering the following expression:

$$converr = \sum_j \left| \frac{Re\left\{f[\hat{n}(\infty),\omega_j]\right\}}{Re\left[\hat{T}_{exp}(\omega_j)\right]} \right| + \left| \frac{Im\left\{f[\hat{n}(\infty),\omega_j]\right\}}{Im\left[\hat{T}_{exp}(\omega_j)\right]} \right|.$$

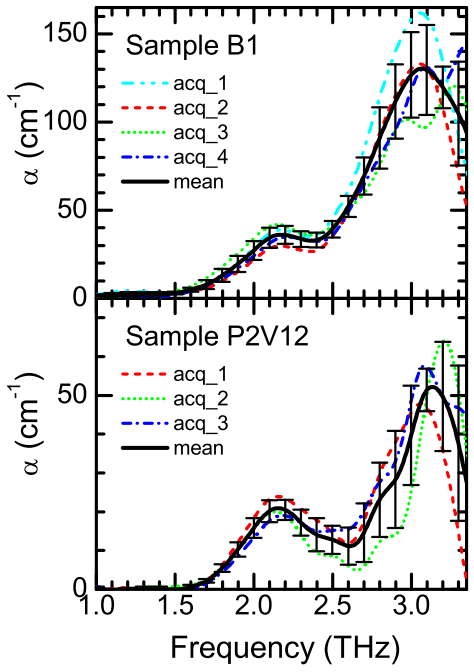

Figure 3. Panels depict the absorption coefficients curves of cellulose fibers obtained by subtracting the backgrounds for each spectrum acquired for samples B1 (acq_1,..., acq_4) and P2V12 (acq_1,..., acq_3). The error bars (spaced by 0.1 THz) indicate the standard deviation of the resulting mean curve (black lines).

The precision of our calculation for the refractive index and absorption coefficient is such that the typical values for *converr* obtained in our application are of the order of 10^{-8}. This implies that the relative difference between any experimental and theoretical transfer function spectral component for the real or imaginary part is, in the worst case, 10^{-8}. The SNR of the FFT amplitude is, at the best, of the order of 10^{-4}. We, therefore, argue that any noise-like feature in the spectra of the extracted optical parameters is likely to have an experimental origin, rather than a numerical or a systematic one.

A numerical low-pass filter (0.14 THz resolution) was then applied to the spectra obtained to cancel the FP contribution and thus eliminate the noise especially present at frequencies higher than 2.5 THz. The typical resulting curve, normalized for both sample thickness and density, is shown in Fig.2 together with a plot where the FP oscillations have not been removed. Note that the FP oscillations can be confused with the spectroscopic features (as shown in the curve in which they are indeed present).

Fig.3 shows examples of measurement uncertainties in the absorption curves from which the background has been subtracted. Although the clearest result is surely the presence of peaks at 2.1 and 3.1 THz , we note that minor peaks systematically occur in the various measurements carried out on the artificially aged samples, thus confirming a modification of the spectra as a function of aging.

* mauro.missori@isc.cnr.it

[1] I. Brueckle, Structure and properties of dry and wet paper, In G. Banik and I. Brueckle, editors, *Paper and Water: A guide for conservators*, chapter 4, pages 81–119, Routledge, London and New York (2011).

[2] M. Missori, O. Pulci, L. Teodonio, C. Violante, I. Kupchak, J. Bagniuk, J. Łojewska, and A. Mosca Conte, Optical response of strongly absorbing inhomogeneous materials: application to paper degradation, Phys. Rev. B **89**, 054201 (2014).

[3] A. F. Mosca Conte, O. Pulci, M. Misiti, J. Łojewska, L. Teodonio, C. Violante, and M. Missori, Visual degradation in Leonardo da Vinci's iconic self-portrait: a nanoscale study, Appl. Phys. Lett. **104**, 224101 (2014).

[4] C. Violante, L. Teodonio, A. Mosca Conte, O. Pulci, I. Kupchak, and M. Missori, An ab-initio approach to cultural heritage: The case of ancient paper degradation, *Physica Status Solidi B* **252**, 112–117 (2015).

[5] A. Mosca Conte, O. Pulci, A. Knapik, J. Bagniuk, R. Del Sole, J. Łojewska, and M. Missori, Role of cellulose oxidation in the yellowing of ancient paper. *Phys. Rev. Lett.* **108**, 158301 (2012).

[6] A. Mosca Conte, O. Pulci, R. Del Sole, A. Knapik, J. Bagniuk, J. Łojewska, L. Teodonio, and M. Missori, Visual degradation in Leonardo da Vinci's iconic self-portrait: a nanoscale study, *e-J. Surf. Sci. Nanotech.* **10**, 569–574 (2012).

[7] T. Łojewski, K. Ziebla, A. Knapik, J. Bagniuk, A. Lubańska, and J. Łojewska, Furfural as a marker of cellulose degradation. a quantitative approach, Appl. Phys. A **100**, 809–821 (2010).

[8] P. Łojewski, P. Miśkowiec, M. Missori, A. Lubańska, L. Proniewicz, and J. Łojewska, Ftir and UV/Vis as methods for evaluation of oxidative degradation of model paper: DFT approach for carbonyl vibrations, Carbohydr. Polym. **82**, 370 (2010).

[9] P. Giannozzi, S. Baroni, N. Bonini, M. Calandra, R. Car, C. Cavazzoni, D. Ceresoli, G.L. Chiarotti, M. Cococcioni, I. Dabo, A. Dal Corso, S. de Gironcoli, S. Fabris, G. Fratesi, R. Gebauer, U. Gerstmann, C. Gougoussis, A. Kokalj, M. Lazzeri, L. Martin-Samos, N. Marzari, F. Mauri, R. Mazzarello, S. Paolini, A. Pasquarello, L. Paulatto, C. Sbraccia, S. Scandolo, G. Sclauzero, P. Ari Seitsonen, A. Smogunov, P. Umari, and R. M. Wentzcovitch, Quantum espresso: a modular and open-source software project for quantum simulations of materials, *Journal of Physics: Condensed Matter* **21**(39), 395502 (2009).

[10] K. Lee, E. D. Murray, L. Kong, B. I. Lundqvist, and D. C. Langreth, Higher-accuracy Van der Waals density functional, Phys. Rev. B **82**, 081101(R) (2010).

[11] M. Dion, H. Rydberg, E. Schroder, D. Langreth, and I. B. Lundqvist, Van der Waals density functional for general geometries, *Phys. Rev. Lett.* **92**, 246401 (2004).

[12] J. Perdew and Y. Wang, Accurate and simple density functional for the electronic exchange energy: Generalized gradient approximation, *Phys. Rev. B* **33**, 8800(R) (1986).

[13] A. K. Kelkkanen, B. I. Lundqvist, and J. K. Norskov, Density functional for van der waals forces accounts for hydrogen bond in benchmark set of water hexamers, *Chem. Phys.* **131**, 046102 (2009).

[14] D. Vanderbilt, Soft self-consistent pseudopotentials in a generalized eigenvalue formalism, *Phys. Rev. B* **41**, 7892(R) (1990).

[15] R. Sabatini, T. Gorni, and S. de Gironcoli, Nonlocal van der waals density functional made simple and efficient, *Phys. Rev. B* **87**, 041108(R) (2013).

[16] A. Calzolari and M. Buongiorno Nardelli, Dielectric properties and Raman spectra of ZnO from a first principles finite-differences/finite-fields approach, *Sci. Rep.* **3**, 2999 (2013).

[17] P. U. Jepsen, D. G. Cooke, and M. Koch, Terahertz spectroscopy and imaging - modern techniques and applications, Laser Photonics Rev. **5** (1), 124–166 (2011).

[18] L. Duvillaret, F. Garet, and J. L. Coutaz, Highly precise determination of optical constants and sample thickness in terahertz time-domain spectroscopy *Appl. Opt.* **38**(2), 409–415 (1999).

[19] L. Duvillaret, F. Garet, and J.-L. Coutaz, A reliable method for extraction of material parameters in terahertz time-domain spectroscopy, *IEEE Journal of Selected Topics in Quantum Electronics* **2**(3), 739 (1996).